

# On the coevolution of Ediacaran oceans and animals

Yanan Shen<sup>\*†</sup>, Tonggang Zhang<sup>\*</sup>, and Paul F. Hoffman<sup>\*†</sup>

<sup>\*</sup>Département des Sciences de la Terre et de l'Atmosphère, Université du Québec, Montréal, QC, Canada H3C 3P8; and <sup>†</sup>Department of Earth and Planetary Sciences, Harvard University, Cambridge, MA 02138

Contributed by Paul F. Hoffman, March 4, 2008 (sent for review December 3, 2007)

**Fe speciation and S-isotope of pyrite data from the terminal Proterozoic Sheepbed Formation in Canada and Doushantuo Formation in China reveal that ocean deep waters were anoxic after the global glaciations (snowball Earth) ending 635 million years ago, but that marine sulfate concentrations and inferentially atmospheric oxygen levels were higher than before the glaciations. This supports a long-postulated link between oxygen levels and the emergence of eumetazoa. Subsequent ventilation of the deep ocean, inferred from shifts in Fe speciation in Newfoundland (previously published data) and western Canada (this report), paved the way for Ediacaran macrobiota to colonize the deep seafloors.**

atmospheric oxygen | iron speciation | sulfur isotopes | Sheepbed Formation | Doushantuo Formation

A pair of global glaciations (1) between 725 and 635 million years ago (Cryogenian Period) was followed by the appearance and diversification of (mainly nonskeletal) multicellular animals in the Ediacaran Period from 635 to 541 million years ago (2–7). The oldest animal fossils include diapause egg and embryo cysts (*Tianzhushania spinosa*) from the lower Doushantuo Formation (≈632 Ma) in South China (8) and lipid biomarkers (24-isopropylcholestane) diagnostic of marine demosponges in late Cryogenian and early Ediacaran strata of Oman (9). In contrast, colonization of the deep seafloor (below the euphotic zone) by large soft-bodied organisms was delayed until mid-Ediacaran time ≈579 Ma (10–14). The delayed appearance of large animals in the fossil record, ≈600 million years after multicellularity arose in algae (15), inspired the hypothesis that an increase in atmospheric oxygen catalyzed early animal evolution (6, 16–22).

Recent chemostratigraphic studies provide some evidence for progressive oxygenation of the Ediacaran ocean (23), including mid-Ediacaran (*ca.* 580 Ma) deep waters (24). The first study based its inference mainly on increasing sulfur isotope fractionation between coexisting sulfides and carbonate-associated sulfate (23); the second was based on the low ratios between highly reactive Fe and total Fe (FeHR/FeT) (24). These data purport to “see” through the veil of diagenesis under the influence of anoxic pore-waters to the redox state of ancient seawater. Here, we present Fe speciation and S-isotope of pyrite data from deep-water ocean-margin settings in northwestern Canada and in South China that point to an extended early Ediacaran interval of sulfate-rich oceans with sulfidic deep waters, implying an oxygen-rich atmosphere, followed by the ventilation of deep waters in mid-Ediacaran time.

## Geological Setting

**Northwest Canada.** Ediacaran strata of the Windermere Supergroup (25) are exposed for >500 km along the concave-to-southwest arc of the Mackenzie Mountains, the topographic expression of the early Cenozoic foreland thrust-fold belt of the northern Canadian Cordillera. Because of a low-angle unconformity with overlying Cambrian strata, the Ediacaran is mainly limited to the Plateau Thrust system, an outcrop belt less than ≈30 km wide. Fortunately, it preserves the shelf-to-slope transition of an Ediacaran passive continental margin (25–27). To the northeast (landward), Ediacaran strata were removed by sub-Cambrian erosion and to the southwest (seaward), they are

mostly buried by younger rocks. Southwest of the Plateau Thrust system, a single transverse structural culmination exposes three separate inliers of Ediacaran strata, the most easterly of which (Sekwi Brook) contains a moderately diverse assemblage of mostly disk-shaped macrofossils, apparently representing the bases of sessile, polypoid, and frond-like, soft-bodied organisms, as well as rare ovate segmented fossils, and abundant simple or irregularly meandering burrows (28–30). The oldest fossils (five genera of disk-shaped forms) occur in the middle Sheepbed Formation (Fig. 1), a 1,050-m-thick sequence of black shales, turbiditic siltstones, and contour-current sands, deposited at estimated water depths of 1–1.5 km on an open-marine continental slope subject to geostrophic currents (26). They are much larger and more diverse than the simple discs found between the two Cryogenian glacial horizons in the same area (31).

The shelf-slope transition is best exposed on Stelfox Mountain (Fig. 1), 25 km northeast of Sekwi Brook, where a major down-to-southwest breakaway paleoscarp (32) marks the outer edge of the Keele Formation, a mixed carbonate-clastic shelf sequence beneath the end-Cryogenian glacial horizon (33). The submarine landslide responsible for the paleoscarp generated an enormous megabreccia, the Durkan Formation (32), carrying house-size blocks of Keele shelf lithologies. The landslide is thought to be unrelated to the subsequent glaciation (32), the retreat of which left a blanket (Stelfox Member) of nonstratified diamictite (marine till) and ice-rafted debris on both the hanging wall and footwall of the paleoscarp (Fig. 1). Stelfox diamictite is overlain by a well developed syn-deglacial “cap” dolostone (Ravensthorpe Formation) with giant wave ripples and corrugate stromatolites, overlain discontinuously by limestone (Hayhook Formation) with seafloor cements (27). At Stelfox Mountain, the dolostone-limestone couplet tapers downslope because of slump-related truncation (Fig. 1). The Ravensthorpe Formation is widely assumed to be correlative with the Nuccaleena cap dolostone at the global stratotype section and point (GSSP) in South Australia, which defines the base of the Ediacaran Period (34, 35).

The basal Ediacaran cap-carbonate couplet is overlain everywhere by a thick black shale, the Sheepbed Formation, which grades into flaggy dark limestones of the overlying Gametrail Formation on Stelfox Mountain (Fig. 1). The shale is associated with long-term flooding of the shelf after the end-Cryogenian (“Marinoan”) glaciation. A stratigraphically and lithologically homologous section of Sheepbed Formation occurs at Shale Lake, 130 km to the northwest. Like Stelfox Mountain, the Shale Lake section is situated on the extreme edge of the Keele shelf (26–28). The Gametrail at Shale Lake is a cliff-forming crystalline dolostone. We elected to measure and sample the Sheepbed

Author contributions: Y.S. and P.F.H. designed research; Y.S., T.Z., and P.F.H. performed research; Y.S. analyzed data; and Y.S. and P.F.H. wrote the paper.

The authors declare no conflict of interest.

Freely available online through the PNAS open access option.

<sup>†</sup>To whom correspondence may be addressed. E-mail: shen.yanan@uqam.ca or hoffman@eps.harvard.edu.

This article contains supporting information online at [www.pnas.org/cgi/content/full/0802168105/DCSupplemental](http://www.pnas.org/cgi/content/full/0802168105/DCSupplemental).

© 2008 by The National Academy of Sciences of the USA



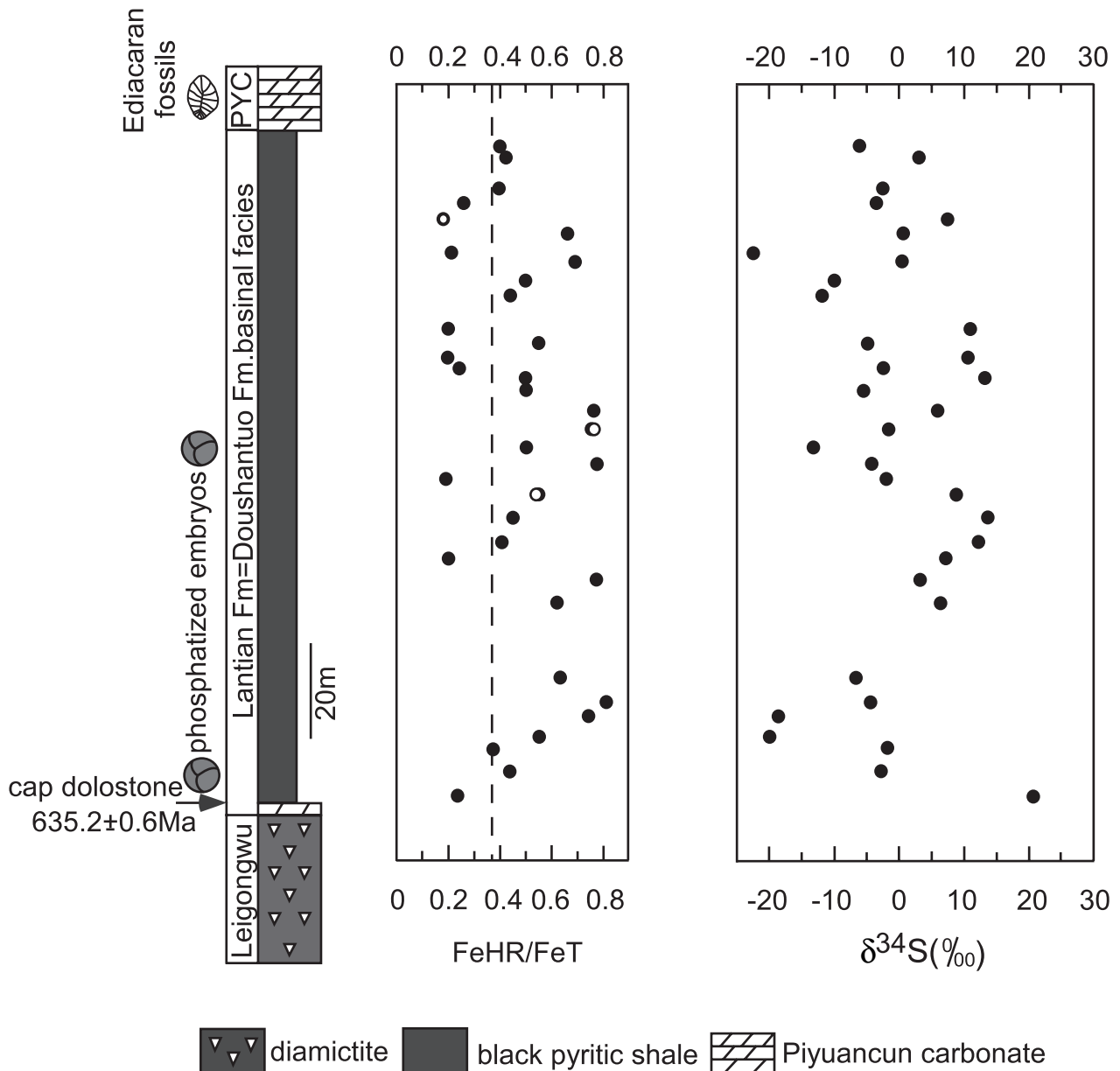


**Fig. 2.** Fe speciation and S-isotopic data from the Lantian Formation, South China. The radiometric age (36) and early animal fossils occur in the correlative Doushantuo and Dengying formations in the oxic shelf succession. Fe speciation data of filled circles were measured by using the method in ref. 47 and the data of open circles were measured by using the method in ref. 52.

whole succession (Fig. 2). The section (Fig. 2) is ≈136 m thick and may represent the thickest basinal succession in the region. It thus records a relatively complete history of deep-water ocean chemistry.

**Results and Discussion**

**Fe Speciation and Oceanic Redox Chemistry.** To reconstruct the redox chemistry of the Ediacaran oceans, various Fe species were measured including dithionite-extractable Fe (FeD), pyrite Fe (FeP), and total Fe (FeT). A paleo-redox proxy (FeHR/FeT), the ratio between highly reactive Fe (FeHR = FeD + FeP) and total Fe (FeT) has been developed to distinguish shales deposited under sulfidic bottom waters from those formed under oxygenated bottom waters. In modern marine sediments, the former have FeHR/FeT ratios typically exceeding 0.38 (47, 48). In contrast, sediments deposited under

oxic bottom waters have FeHR/FeT ratios of <0.38 (47, 48). The Fe speciation criterion has been successfully tested in ancient (Mesozoic) fine-grained sediments where oxic bottom waters are independently indicated by the presence and diversity of oxygen-requiring benthic fauna, and by the disruption of sedimentary layering (bioturbation) resulting from their feeding activities (49). Fe speciation analyses are most useful in Precambrian sediments deposited before animals had evolved (24, 50–52). The elevated FeHR/FeT ratios of sediments deposited in anoxic basins may result from the formation of pyrite in sulfidic water columns in addition to that formed during diagenesis. The source of water-column Fe is probably either the reduction of Fe oxides in basin margin sediments impinged on by the anoxic water column or Fe oxide-containing particles falling through the water column (47, 48, 50, 53).



**S-isotope and Oceanic Sulfate Concentration.** Sulfate concentrations inferred from S-isotopic records are an excellent tracer of atmospheric oxygen levels (e.g., 60–64). To reconstruct their concentrations in late Neoproterozoic oceans, S-isotopic compositions of pyrites in sedimentary rocks of the Sheepbed and Lantian formations were measured. S-isotopic compositions of pyrite in the lower Sheepbed Formation range from  $-23.1$  to  $+27.3‰$  (see also ref. 60 with four S-isotopic analyses ranging from  $-12.6$  to  $+22.6‰$ ) (Fig. 1). Pyrites in the oxic sediments of the upper Sheepbed Formation show a similar wide range of  $\delta^{34}\text{S}$  values from  $-22.5$  to  $+44.8‰$  (Fig. 1). Likewise, pyrites in the Lantian black shales are characterized by  $\delta^{34}\text{S}$  values from  $-21.9$  to  $+20.9‰$  (Fig. 2).

The S-isotopic data of pyrites from both the lower Sheepbed and Lantian formations show significant  $^{34}\text{S}$ -depleted values relative to coeval seawater sulfate with a probable isotopic value of  $+30$ – $35‰$  (65) (Figs. 1 and 2). These isotopic records are consistent with sulfidic depositional environments where pyrite formation in the water columns and sediments are often not limited by sulfate availability and are therefore  $^{34}\text{S}$ -depleted. However, the S-isotopic data of pyrites from oxic upper Sheepbed Formation also show  $^{34}\text{S}$ -depleted values comparable to those from the lower sulfidic sediments and the basal Lantian Formation (Figs. 1 and 2). The same pattern is seen when we compare S-isotopic data from the sulfidic Lantian Formation in China ranging from  $-21.9$  to  $+20.9‰$  and the correlative Pertatataka Formation deposited under oxic normal marine conditions in Australia with  $\delta^{34}\text{S}$  values from  $-22.0$  to  $+34.1‰$  (66). Thus, intra- and interbasinal correlations suggest that the late Ediacaran S-isotopic records of pyrites are not sensitive to changes in water-column redox chemistry.

S-isotopic patterns of pyrites that are independent of water-column redox chemistry have been observed from numerous Phanerozoic anoxic marine basins, arguably as a result of high oceanic sulfate concentrations in an oxygen-rich Phanerozoic world (60, 67). Under sulfate-rich conditions, most diagenetic pyrites in oxic sediments are formed near the redox boundary within the sediments where sulfate depletions are minimal. Therefore,  $\delta^{34}\text{S}$  value of seawater sulfate is inherited in near-surface pore waters, producing a wide range of  $^{34}\text{S}$ -depleted isotopic values as observed in many Phanerozoic rocks (e.g., 67).

Pyrites in the oxic upper Sheepbed Formation exhibit comparable  $^{34}\text{S}$ -depleted isotopic values (down to  $-22.5‰$ ) to those

in the sulfidic Lantian and lower Sheepbed formations (down to  $-23.1‰$ ) (Figs. 1 and 2). A few pyrites ( $n = 4$ ) in the oxic upper Sheepbed with exceptionally positive values heavier than seawater sulfate ( $+30$ – $35‰$ ) could have resulted from rare sulfate depletion in the sediments and/or methane-driven sulfate reduction (68). Regardless, the Sheepbed and Lantian formations display Phanerozoic-type S-isotopic fractionations. Therefore, they provide strong evidence for sulfate-rich conditions in the Ediacaran oceans and, by implication, elevated atmospheric oxygen. However, the early Ediacaran ocean was sulfidic, evidenced by our Fe speciation data, suggesting that sulfate concentrations had not yet reached the levels of modern oceans ( $\approx 28$  mM) and that atmospheric oxygen was below present levels.

## Conclusions

Low oceanic sulfate concentrations during the Proterozoic have been documented by S-isotopic records of pyrite (50–52, 60, 61), trace sulfate (69–72), calculations of the Proterozoic hydrothermal fluid compositions (73), and measurements of multiple S-isotopes on trace sulfate in Proterozoic carbonate (74). The low sulfate concentrations persisted until the end-Cryogenian (635 Ma) snowball glaciation (66, 75). The S-isotopic records from the Lantian and Sheepbed formations indicate a rise in sulfate and therefore atmospheric oxygen concentrations to levels intermediate between the earlier Proterozoic and the present day. This is consistent with the findings of Halverson and Hurtgen (2007) and with the metabolic and collagen-synthesis requirements of eumetazoa in oxic surface waters of the Doushantuo shelf. Early Ediacaran oxygen levels were insufficient, however, to oxidize the deep oceans. Deep-sea ventilation, recorded by the shift in FeHR/FeT ratios in Newfoundland (24) and western Canada (Fig. 1), occurred later,  $\approx 580$  Ma in Newfoundland, allowing large organisms to flourish for the first time on the deep seafloor.

**ACKNOWLEDGMENTS.** We thank Boswell Wing and Shuhai Xiao for constructive comments and Robert Dalrymple for discussions on the Sheepbed sedimentology. This work was supported by Canada Research Chairs Program, Natural Sciences and Engineering Research Council, and in part by the National Aeronautics and Space Administration Astrobiology Institute (Y.S.). Fieldwork in Canada was supported by National Science Foundation Grant EAR-9905495 (to P.F.H.). P.F.H. was also supported by the Canadian Institute for Advanced Research and from Harvard University. The Gametrail C-isotopes were measured by Francis A. Macdonald and Greg Eiseheid from micro-drilled samples in the Harvard University Laboratory for Geochemical Oceanography according to methods described in ref. 58.

- Hoffman PF, Schrag DP (2002) The snowball Earth hypothesis: Testing the limits of global change. *Terra Nova* 14:129–155.
- Harland WB, Rudwick MJS (1964) The great infra-Cambrian ice age. *Sci Am* 211:28–36.
- Gehling JG, Rigby KJ (1996) Long expected sponges from the Neoproterozoic Ediacara fauna of South Australia. *J Paleontol* 70:185–195.
- Fedonkin MA, Waggoner BM (1997) The Late Precambrian fossil *Kimberella* is a mollusc-like bilaterian organism. *Nature* 388:868–871.
- Xiao S, Zhang Y, Knoll AH (1998) Three-dimensional preservation of algae and animal embryos in a Neoproterozoic phosphorite. *Nature* 391:553–558.
- Knoll AH, Carroll SB (1999) The early evolution of animals: Emerging views from comparative biology and geology. *Science* 284:2129–2137.
- Fedonkin MA (2003) The origin of the Metazoa in the light of the Proterozoic fossil record. *Paleontol Res* 7:9–41.
- Yin L, et al. (2007) Doushantuo embryos preserved inside diapause egg cysts. *Nature* 446:661–663.
- Love GD, et al. (2006) Constraining the timing of basal metazoan radiation using molecular biomarkers and U-Pb isotope dating. *Geochim Cosmochim Acta (Goldschmidt Conf Abstr Suppl)* 70:A371.
- Narbonne GM, Gehling JG (2003) Life after snowball: The oldest complex Ediacaran fossils. *Geology* 31:27–30.
- Bowring SA, Myrow P, Landing E, Ramenzani J (2003) Geochronological constraints on terminal Neoproterozoic events and the rise of Metazoans. *NASA Astrobiol Inst (NAI Gen Mtg Abstr)* 2003:113–114.
- Wood DA, Dalrymple RW, Narbonne GM, Gehling JG, Clapham ME (2003) Paleoenvironmental analysis of the late Neoproterozoic Mistaken Point and Trepassy formations, southeastern Newfoundland. *Can J Earth Sci* 40:1375–1391.
- Narbonne GM (2005) The Ediacara biota: Neoproterozoic origin of animals and their ecosystems. *Annu Rev Earth Planet Sci* 33:421–442.
- Bottjer DJ, Clapham ME (2006) Evolutionary paleoecology of Ediacaran benthic marine animals. *Neoproterozoic Geobiology and Paleobiology*, eds Xiao S, Kaufman AJ (Springer, Dordrecht, Netherlands), pp 91–114.
- Butterfield NJ (2000) *Bangiomorpha pubescens* n. gen., n. sp.: Implications for the evolution of sex, multicellularity, and the Mesoproterozoic/Neoproterozoic radiation of eukaryotes. *Paleobiology* 26:386–404.
- Nursall JR (1959) Oxygen as a prerequisite to the origin of the Metazoa. *Nature* 183:1170–1172.
- Berkner LV, Marshall J (1965) On origin and rise of oxygen concentration in Earth's atmosphere. *J Atmos Sci* 22:225–261.
- Towe KM (1970) Oxygen-collagen priority and early metazoan fossil record. *Proc Natl Acad Sci USA* 65:781–788.
- Cloud P (1972) Working model of primitive Earth. *Am J Sci* 272:537–548.
- Runnegar B (1982) Oxygen requirements, biology and phylogenetic significance of the late Precambrian worm Dickinsonia, and the evolution of the burrowing habit. *Alcheringa* 6:223–239.
- Graham JB (1988) Ecological and evolutionary aspects of integumentary respiration: Body size, diffusion, and the Invertebrata. *Am Zool* 28:1031–1045.
- Knoll AH, Hayes JM, Kaufman AJ, Swett K, Lambert IB (1986) Secular variation in carbon isotope ratios from Upper Proterozoic successions of Svalbard and East Greenland. *Nature* 321:832–838.
- Fike DA, Grotzinger JP, Pratt LM, Summons RE (2006) Oxidation of the Ediacaran Ocean. *Nature* 444:744–747.
- Canfield DE, Poulton SW, Narbonne GM (2007) Late-Neoproterozoic deep-ocean oxygenation and the rise of animal life. *Science* 315:92–95.

25. Narbonne GM, Aitken JD (1995) Neoproterozoic of the Mackenzie Mountains, northwestern Canada. *Precambrian Res* 73:101–121.
26. Dalrymple RW, Narbonne GM (1996) Continental slope sedimentation in the Sheepbed Formation (Neoproterozoic, Windermere Supergroup), Mackenzie Mountains, N.W.T. *Can J Earth Sci* 33:848–862.
27. James NP, Narbonne GM, Kyser TK (2001) Late Neoproterozoic cap carbonates: Mackenzie Mountains, northwestern Canada: Precipitation and global glacial meltdown. *Can J Earth Sci* 38:1229–1262.
28. Aitken JD (1989) Uppermost Proterozoic formations in central Mackenzie Mountains, Northwest Territories. *Geol Surv Can Bull* 368:1–26.
29. Narbonne GM, Aitken JD (1990) Ediacaran fossils from the Sekwi Brook area, Mackenzie Mountains, Northwestern Canada. *Palaeontology* 33:945–980.
30. Narbonne GM (1994) New Ediacaran fossils from the Mackenzie Mountains, Northwestern Canada. *J Paleont* 68:411–416.
31. Hofmann HJ, Narbonne GM, Aitken JD (1990) Ediacaran remains from intertillite beds in Northwestern Canada. *Geology* 18:1199–1202.
32. Aitken JD (1991) The Ice Brook Formation and post-Rapitan, Late Proterozoic glaciation, Mackenzie Mountains, Northwest Territories. *Geol Surv Can Bull* 404:1–43.
33. Day ES, James NP, Narbonne GM, Dalrymple RW (2004) A sedimentary prelude to Marinoan glaciation, Cryogenian (Middle Neoproterozoic) Keele Formation, Mackenzie Mountains, northwestern Canada. *Precambrian Res* 133:223–247.
34. Knoll AH, Walter MR, Narbonne GM, Christie-Blick N (2006) The Ediacaran Period: A new addition to the geologic time scale. *Lethaia* 39:13–30.
35. Halverson GP (2006) A neoproterozoic chronology. *Neoproterozoic Geobiology and Paleobiology*, eds Xiao S, Kaufman AJ (Springer, Dordrecht, Netherlands), pp 231–271.
36. Condon D, et al. (2005) U-Pb ages from the Neoproterozoic Doushantuo Formation, China. *Science* 308:95–98.
37. Sun WG (1986) Late Precambrian pennatulids (sea pens) from the eastern Yangtze Gorge, China: *Paracharnia* gen. nov. *Precambrian Res* 31:361–375.
38. Xiao S, Shen B, Zhou C, Yuan X (2005) A uniquely preserved Ediacaran fossil with direct evidence for a quilted bodyplan. *Proc Natl Acad Sci USA* 102:10227–10232.
39. Li C, Chen JY, Hua T (1998) Precambrian sponges with cellular structures. *Science* 279:879–882.
40. Yuan X, Hofmann HJ (1998) New microfossils from the Neoproterozoic (Sinian) Doushantuo Formation, Wengan, Guizhou Province, southwestern China. *Alcheringa* 22:189–222.
41. Xiao S, Yuan X, Knoll AH (2000) Eumetazoan fossils in terminal Proterozoic phosphorites? *Proc Natl Acad Sci USA* 97:13684–13689.
42. Xiao S, Knoll AH (2000) Phosphatized animal embryos from the Neoproterozoic Doushantuo Formation at Weng'an, Guizhou, South China. *J Paleont* 74:767–788.
43. Chen JY, et al. (2004) Small bilaterian fossils from 40 to 55 million years before the Cambrian. *Science* 305:218–222.
44. Zhu M, Zhang J, Yang A (2007) Integrated Ediacaran (Sinian) chronostratigraphy of South China. *Palaeogeogr Palaeoclimatol Palaeoecol* 254:7–61.
45. Chen M, Lu G, Xiao Z (1994) Preliminary study on the algal macrofossils—Lantian Flora from the Lantian Formation of Upper Sinian in southern Anhui. *Bull Inst Geol Acad Sinica* 7:252–267.
46. Yan Y, Jiang C, Zhang S, Du S, Bi Z (1992) Research of the Sinian System in the region of western Zhejiang, northern Jiangxi, and southern Anhui provinces. *Bull Nanjing Inst Geol Miner Resour Chinese Acad Geol Sci* 12:1–105.
47. Raiswell R, Canfield DE (1998) Sources of iron for pyrite formation in marine sediments. *Am J Sci* 298:219–245.
48. Lyons TW, Severmann S (2006) A critical look at iron paleoredox proxies based on new insights from modern euxinic marine basins. *Geochim Cosmochim Acta* 70:5698–5722.
49. Raiswell R, Newton R, Wignall PB (2001) An indicator of water-column anoxia: Resolution of biofacies variations in the Kimmeridge Clay (Upper Jurassic, UK). *J Sediment Res* 71:286–294.
50. Shen Y, Canfield DE, Knoll AH (2002) Middle Proterozoic ocean chemistry: Evidence from the McArthur Basin, northern Australia. *Am J Sci* 302:81–109.
51. Shen Y, Knoll AH, Walter MR (2003) Evidence for low sulphate and anoxia in a mid-Proterozoic marine basin. *Nature* 423:632–635.
52. Poulton SW, Fralick PW, Canfield DE (2004) The transition to a sulfidic ocean  $\approx 1.84$  billion years ago. *Nature* 431:173–177.
53. Wijsman JWM, Middleburg JJ, Herman PMJ, Böttcher ME, Heip CHR (2001) Sulfur and iron speciation in surface sediments along the northwestern margin of the Black Sea. *Mar Chem* 74:261–278.
54. Narbonne GM, Kaufman AJ, Knoll AH (1994) Integrated chemostratigraphy and biostratigraphy of the Windermere Supergroup, Northwestern Canada—Implications for Neoproterozoic correlations and the early evolution of animals. *Geol Soc Am Bull* 106:1281–1292.
55. Kaufman AJ, Knoll AH, Narbonne GM (1997) Isotopes, ice ages, and terminal Proterozoic earth history. *Proc Natl Acad Sci USA* 94:6600–6605.
56. Burns SJ, Matter A (1993) Carbon isotopic record of the latest Proterozoic from Oman. *Eclogae Geol Helv* 86:595–607.
57. Le Guerroué E, Allen PA, Cozzi A, Etienne JL, Fanning M (2006) 50 Myr recovery from the largest negative  $\delta^{13}\text{C}$  excursion in the Ediacaran ocean. *Terra Nova* 18:147–153.
58. Halverson GP, Hoffman PF, Schrag DP, Maloof AC, Rice AHN (2005) Toward a Neoproterozoic composite carbon-isotope record. *Geol Soc Am Bull* 117:1181–1207.
59. Zhou C, Xiao S (2007) Ediacaran  $\delta^{13}\text{C}$  chemostratigraphy of South China. *Chem Geol* 237:89–108.
60. Hayes JM, Lambert IB, Strauss H (1992) The sulfur-isotopic record. *The Proterozoic Biosphere: A Multidisciplinary Study*, eds Schopf JW, Klein C (Cambridge Univ Press, Cambridge, UK), pp 129–132.
61. Canfield DE (1998) A new model for Proterozoic ocean chemistry. *Nature* 396:450–453.
62. Strauss H (2002) The isotopic composition of Precambrian sulphides—seawater chemistry and biological evolution. *Precambrian Sedimentary Environments: A Modern Approach to Ancient Depositional Systems*, eds Altermann W, Corcoran PL (Blackwell Science, Oxford, UK), pp 67–105.
63. Shen Y, Buick R (2004) The antiquity of microbial sulfate reduction. *Earth-Sci Rev* 64:243–272.
64. Halverson GP, Hurtgen MT (2007) Ediacaran growth of the marine sulfate reservoir. *Earth Planet Sci Lett* 263:32–44.
65. Goldberg T, Poulton SW, Strauss H (2005) Sulphur and oxygen isotope signatures of late Neoproterozoic to early Cambrian sulphate, Yangtze Platform, China: Diagenetic constraints and seawater evolution. *Precambrian Res* 137:223–241.
66. Gorjan P, Veevers JJ, Walter MR (2000) Neoproterozoic sulfur-isotope variation in Australia and global implications. *Precambrian Res* 100:151–179.
67. Logan GA, Hayes JM, Hieshima GB, Summons R (1995) Terminal Proterozoic reorganization of biogeochemical cycles. *Nature* 376:53–56.
68. Jørgensen BB, Böttcher ME, Lüschen H, Neretin LN, Volkov II (2004) Anaerobic methane oxidation and a deep  $\text{H}_2\text{S}$  sink generate isotopically heavy sulfides in Black Sea sediments. *Geochim Cosmochim Acta* 68:2095–2118.
69. Kah LC, Lyons TW, Frank TD (2004) Low marine sulphate and protracted oxygenation of the Proterozoic biosphere. *Nature* 431:834–838.
70. Gellatly AM, Lyons TW (2005) Trace sulfate in mid-Proterozoic carbonates and the sulfur isotope record of biospheric evolution. *Geochim Cosmochim Acta* 69:3813–3829.
71. Hurtgen MT, Arthur MA, Halverson GP (2005) Neoproterozoic sulfur isotopes, the evolution of microbial sulfur species, and the burial efficiency of sulfide as sedimentary pyrite. *Geology* 33:41–44.
72. Hurtgen MT, Halverson GP, Arthur MA, Hoffman PF (2006) Sulfur cycling in the aftermath of a 635-Ma snowball glaciation: Evidence for a syn-glacial sulfidic deep ocean. *Earth Planet Sci Lett* 245:551–570.
73. Kump LR, Seyfried WE (2005) Hydrothermal Fe fluxes during the Precambrian: Effect of low oceanic sulfate concentrations and low hydrostatic pressure on the composition of black smokers. *Earth Planet Sci Lett* 235:654–662.
74. Johnston DT, et al. (2005) Active microbial sulfur disproportionation in the Mesoproterozoic. *Science* 310:1477–1479.
75. Hurtgen MT, Arthur MA, Suits NS, Kaufman AJ (2003) The sulfur isotopic composition of Neoproterozoic seawater sulfate: Implications for a snowball Earth? *Earth Planet Sci Lett* 203:413–429.